Supporting Information

Compound-Specific Stable Isotope Fractionation of Pesticides and Pharmaceuticals in a Mesoscale Aquifer Model

Heide K. V. Schürner,[†] *Michael P. Maier,*[†] *Dominik Eckert,*[‡] *Ramona Brejcha,*[†] *Claudia-Constanze Neumann,*[†] *Christine Stumpp,*[†] *Olaf A. Cirpka,*[‡] *Martin Elsner*[†,*]

[†]Institute of Groundwater Ecology, Helmholtz Zentrum München, Ingolstädter Landstraße 1, 85764 Neuherberg, Germany

[‡] Center for Applied Geosciences, University of Tübingen, Hölderlinstraße 12, 72074 Tübingen, Germany

*Corresponding author: Phone: +49 (0)89 31872565; fax: +49 (0)89 31873361;

e-mail: martin.elsner@helmholtz-muenchen.de

Contains:

Pages: 18

Figures: 4

Tables: 3

Contents:

1. Experimental Section

1.1. Chemicals

BAM (2,6-dichlorobenzamide, CAS: 2008-58-4, 99.9%), bentazone (3-*iso*-propyl-(1*H*)-2,1,3-benzothiadiazin-4(3*H*)-one 2,2-dioxide, CAS: 25057-89-0, 99.9%), diclofenac (2-[(2,6-dichlorophenyl)amino]benzeneacetic acid sodium salt, CAS: 15307-79-6), and ibuprofen ((*RS*)-2-[4-(2-methylpropyl)phenyl]propanoic acid, CAS: 15687-27-1, $\geq 98\%$) were purchased from Sigma-Aldrich (Steinheim, Germany). D_2O (90 atom % D) was from Berlin-Chemie (Berlin-Adlershof, Germany). BF_3 (10% in methanol) was purchased from Sigma-Aldrich (Steinheim, Germany), TMSH (trimethylsulfonium hydroxide, 0.25 M in methanol) was from Fluka, supplied by Sigma-Aldrich (Steinheim, Germany). HCl (32%) and KBr were from Merck (Darmstadt, Germany), H_3PO_4 (85%) and NaOH were from Sigma-Aldrich (Steinheim, Germany). Milli-Q water was generated by a Milli-Q Advantage $A10_{system}$ (Millipore, Schwalbach, Germany). Acetonitrile and ethyl acetate were from Fluka, supplied by Sigma-Aldrich (Taufkirchen, Germany), acetic acid (0.1% in water), *n*-hexane, and methanol were purchased from Carl Roth (Karlsruhe, Germany) and were of LC-MS grade (purity > 99%).

1.2. Quantification with LC-MS/MS

Concentrations of BAM, bentazone, diclofenac, 4'-hydroxydiclofenac, ibuprofen, and 2-hydroxyibuprofen were measured on an LC-MS/MS system consisting of an Agilent 1200 binary pump (Agilent Technologies, Böblingen, Germany) and an ABSciex API 2000 Q-TRAP mass spectrometer (Applied Biosystems, Framingham, USA). A Luna C18(2) column (5 µm, 100 × 2 mm) purchased from Phenomenex (Aschaffenburg, Germany) was used. Liquid samples (25 µL) were injected with a GC Pal autosampler (CTC Analytics, Zwingen, Switzerland). The peaks were separated by gradient elution starting with 4%

acetonitrile and 96% acetic acid (0.1% in water) isocratic for 2 min at a constant flow rate of 0.3 mL/min. The gradient increased linearly within 28 min to 90% acetonitrile (hold 2 min), before initial conditions were reached within 8 min. Ionization was achieved with positive (0-12 min) and negative (12-40 min) electrospray ionization in multi reaction mode (MRM). The screened molecular and fragment masses are shown in Table S1.

Table S1. Overview of the LC-MS/MS settings used for quantification of 2,6-dichlorobenzamide (BAM), bentazone, diclofenac (Dic), 4'-hydroxydiclofenac (4'-OH-Dic), ibuprofen (Ibu), and 2-hydroxyibuprofen (2-OH-Ibu). $^{13}C_6$-diclofenac ($^{13}C_6$-Dic) and ibuprofen-d_3 (Ibu-d_3) were used as internal standards.

	BAM	**bentazone**	**Dic/ $^{13}C_6$-Dic**	**4'-OH-Dic**	**Ibu/ Ibu-d_3**	**2-OH-Ibu**
molecular mass [M-H]$^+$	190	-	-	-	-	-
fragment mass [M-H]$^+$	145	-	-	-	-	-
molecular mass [M-H]$^-$	-	239	294/300	310	205/208	221
fragment mass [M-H]$^-$	-	132	250/256	266	161/164	177
declustering potential	41	-26	-16	-16	-10	-10
extraction potential	8	-5.5	-6	-7.5	-6	-6
collision energy	35	-32	-12	-12	-12	-12
cell exit potential	4	0	-2	-4	-2	-2
ion spray voltage [V]	+5500	-4500	-4500	-4500	-4500	-4500
source temperature [°C]	350	350	350	350	350	350

1.3. Sample Enrichment with SPE

To enrich the samples, solid phase extraction (SPE) was performed with a vacuum chamber (Macherey-Nagel, Düren, Germany) equipped with Oasis® HLB extraction cartridges (6 cm^3, 200 mg) purchased from Waters (Milford, USA). Stored samples were adjusted to pH 7 with 1 M HCl. First, the cartridges were conditioned (2 × 4 mL methanol, 2 × 4 mL Milli-Q water), then samples were loaded (flow: ~3 mL/min). Afterwards, the sorbent was washed with Milli-Q water (4 mL) and dried under vacuum. To elute the target compounds, methanol (2 × 4 mL) was used. The organic solvent was evaporated under the fume hood with a gentle nitrogen stream and the samples were redissolved in methanol (3 × 500 µL).

1.4. Preparative HPLC

Preparative HPLC was performed using an LC-A10 series HPLC system (Shimadzu, Kyōto, Japan) equipped with a fraction collector. The column was an Allure C18 (5 µm, 150 × 4.6 mm) from Restek (Bad Homburg, Germany). Peak separation was conducted using gradient elution with a flow rate of 0.8 mL/min. The oven temperature was set to 35 °C. Initial eluent conditions were 10% acetonitrile and 90% H_3PO_4 (5 mM, pH 2) isocratic for 1 min, then increasing linearly to 30% acetonitrile within 5 min followed by a linear gradient to 50% acetonitrile within 5 min (hold 3 min). After another linear increase to 70% acetonitrile within 4 min (hold 2 min), initial conditions were reached within 3 min. The sample volume was ~330 µL (three measurements per sample) injected manually into a 500 µL loop. Compounds were detected by UV absorbance at 220 nm. Fractions with a volume of 1 mL each were collected between 5-26.5 min. Vials containing the same substance were combined and the solvent was evaporated under the fume hood with a gentle nitrogen stream.

1.5. Isotope Analysis – $\delta^{13}C$ and $\delta^{15}N$ Analysis of BAM, Bentazone, and Diclofenac

Carbon and nitrogen isotope analysis of BAM, bentazone, and diclofenac was carried out on a GC-IRMS system consisting of a TRACE GC Ultra gas chromatograph (Thermo Fisher Scientific, Milan, Italy) equipped with a DB-5 analytical column (30 m, 0.25 mm ID, 1.0 µm film, Agilent Technologies, Böblingen, Germany). The GC was coupled to a Finnigan MAT 253 isotope ratio mass spectrometer via a Finnigan GC Combustion III interface (both Thermo Fisher Scientific, Bremen, Germany). Liquid samples were injected with a GC Pal autosampler (CTC Analytics, Zwingen, Switzerland). Analysis of the contaminants was done with established in-house methods.[1-3] While BAM was analyzed without further modification, online derivatization by TMSH and offline derivatization by methanolic BF_3 was necessary prior to analysis of bentazone and diclofenac, respectively.

In short, the split/splitless injector (250 °C, He carrier flow rate: 1.4 mL/min) used for BAM analysis was operated in splitless mode for 2 min, then in split mode (split ratio 1:10). Initial GC oven temperature was 120 °C (hold 1 min), ramped with 8 °C/min to 200 °C (hold 2 min), and ramped with 15 °C/min to 280 °C (hold 2 min).

Bentazone was derivatized online with trimethylsulfonium hydroxide (TMSH) in a programmable GC injector (Optic 3-SG High Power Injection System, ATAS GL Sciences B.V., previously ATAS GL International B.V., Eindhoven, The Netherlands) equipped with a packed glassbead liner. Initial injector temperature was 40 °C and the column flow was set to 1.4 mL/min. After a vent time of 5 min with a split flow of 50 mL/min, the split flow was set to 0 mL/min for 3.5 min, while the injector was ramped with 14 °C/min to 250 °C. The GC program began at 80 °C (hold 1 min), ramped with 20 °C/min to 190 °C, and ramped with 8 °C/min to 260 °C (hold 5 min).

Diclofenac was derivatized offline with BF_3/methanol prior to analysis and injected into the programmable GC injector already mentioned above. The injector was equipped with an on-column liner connected directly to a retention gap (FS-methyl-silyl, 3 m, 0.53 mm ID, Chromatographie Service GmbH, Langerwehe, Germany). The initial injector temperature was 40 °C (hold 4 min), ramped with 17 °C/min to 200 °C, while the column flow was set to 0.3 mL/min (hold 2 min), ramped to 1.4 mL/min within 2 min. A constant split ratio of 1:10 was used. The initial GC oven temperature was 40 °C (hold 4 min), ramped with 17 °C/min to 200 °C (hold 3 min), and ramped with 15 °C/min to 260 °C (hold 20 min).

Derivatization (in this case methylation) changes the bulk carbon isotope ratio by introduction of an additional carbon atom. To keep the resulting δ^{13}C-shift constant, the same batch of TMSH and BF_3/methanol, respectively, was used for all samples. To correct for the introduced methyl group, the following equation was used[4]

$$\delta^{13}C_{\mathrm{sample}} = \frac{(n+1)\times\delta^{13}C_{\mathrm{analyte-Me}}-\delta^{13}C_{\mathrm{Me}}}{n} \tag{S.1}$$

where n is the number of carbon atoms present in the analyte (bentazone: $n = 10$; diclofenac: $n = 14$), $\delta^{13}C_{\text{analyte-Me}}$ and $\delta^{13}C_{\text{Me}}$ are the isotope ratios of the derivatized analyte (measured) and the introduced methyl group, respectively, that, in turn, can be calculated according to:

$$\delta^{13}C_{\mathrm{Me}} = (n+1)\times\delta^{13}C_{\mathrm{analyte-Me}} - n\times\delta^{13}C_{\mathrm{EA-IRMS}} \tag{S.2}$$

$\delta^{13}C_{\text{EA-IRMS}}$ is the carbon isotope ratio of the lab standard that was determined prior to derivatization on an EuroEA elemental analyzer (EuroVector, Milan, Italy) coupled to a Finnigan MAT253 IRMS by a FinniganConFlow III interface (both Thermo Fisher Scientific, Bremen, Germany) and calibrated against organic reference materials (USGS 40, USGS 41, IAEA 600, IAEA CH6) provided by the International Atomic Energy Agency (IAEA, Vienna).

2. Results and Discussion

2.1. Breakthrough Curves of BAM, Bentazone, Diclofenac, Ibuprofen, and Conservative Tracer D_2O.

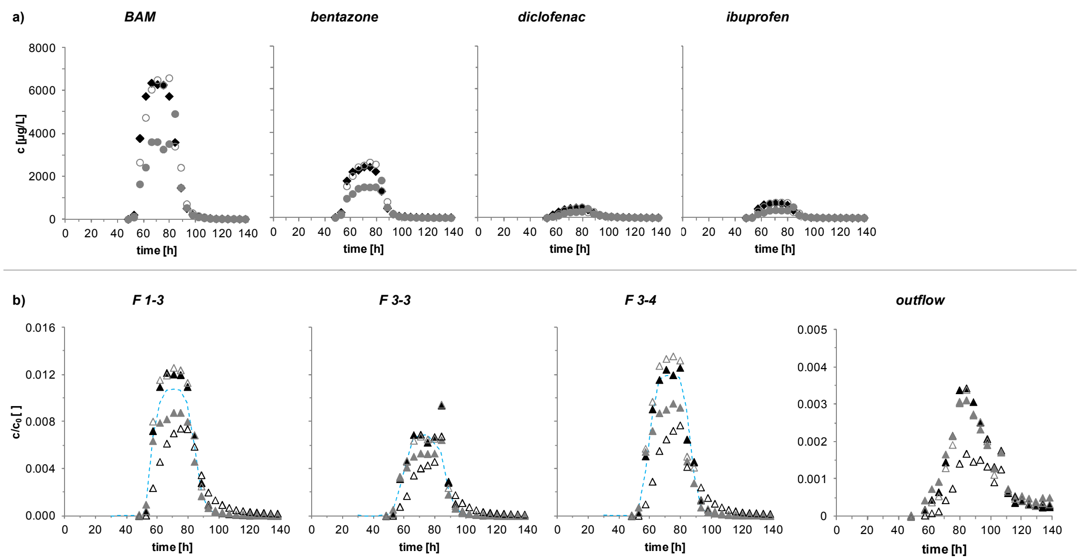

Figure S1. Breakthrough curves of BAM, bentazone, diclofenac, and ibuprofen. (a) Absolute concentrations of contaminants measured in sampling ports F 1-3 (black diamonds), F 3-3 (gray dots), and F 3-4 (gray open dots). (b) Relative concentrations of BAM (black triangles), bentazone (gray triangles), diclofenac (black open triangles), and ibuprofen (gray open triangles) in each sampling port and in the aquifer outflow compared to D_2O (blue dashed line). Tracer data of the outflow was not analyzed. Note that the resolution of the outflow data is not as high as that of the sampling ports, because the various flow paths of the system are combined.

2.2. Recovery and Isotopic Mass Balance of Bentazone and Diclofenac

The isotopic mass balances were calculated according to the Rayleigh equation

$$ln\left(\frac{\overline{\delta\ ^{h}E}+1}{\delta\ ^{h}E_0+1}\right) = \varepsilon \times lnf \tag{S.3}$$

with ε being the enrichment factor and f the fraction of the remaining substrate. The weighted average $\overline{\delta\ ^{h}E}$ of the isotopic signature $\delta^{h}E_i$ (i.e., $\delta^{13}C$ and $\delta^{15}N$, respectively) is given as

$$\overline{\delta\ ^{h}E} = \frac{\sum_{i=1}^{n}\left(\delta\ ^{h}E_i \times V_i \times c_i\right)}{\sum_{i=1}^{n}(V_i \times c_i)} \tag{S.4}$$

where V_i is the sample volume and c_i is the respective sample concentration at time i.

Table S2. Recoveries and Isotopic Mass Balances of Bentazone and Diclofenac in the Sampling Ports F 1-3, F 3-3, and F 3-4.

	bentazone				**diclofenac**			
	1-3	**3-3**	**3-4**	**average**	**1-3**	**3-3**	**3-4**	**average**
recovery [%]	69.7	74.0	74.1	72.6 ± 2.5	61.2	62.3	59	60.8 ± 1.7
degradation [%]	30.3	26.0	25.9	27.4 ± 2.5	38.8	37.7	41.0	39.2 ± 1.7
δ^{13}C mass balance [%]	-	-	-	-	83.5	80.6	52.2	72.1 ± 17.3
δ^{15}N mass balance [%]	93.5	84.8	70.7	83.0 ± 11.5	63.5	82.7	59.0	68.4 ± 12.6
δ^{13}C difference between weighted av and input [‰]	-	-	-	-	0.4	0.4	1.3	0.7 ± 0.5
δ^{15}N difference between weighted av and input [‰]	0.7	1.7	3.5	1.9 ± 1.4	3.2	1.3	3.7	2.7 ± 1.3

2.3. Breakthrough Curves of Diclofenac and its Metabolite 4'-Hydroxydiclofenac

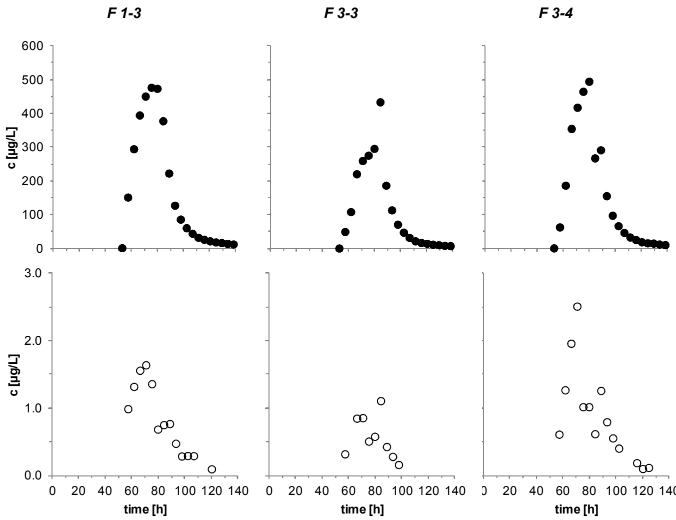

Figure S2. Absolute concentrations of diclofenac (filled dots) and its metabolite 4'-hydroxydiclofenac (open dots).

3. Mathematical Model

3.1. Solute Transport Undergoing First-Order Degradation and Mass Exchange

The traditional notation of multi-dimensional advective-dispersive transport of a compound undergoing linear, one-site, kinetic sorption and first-order decay reads as:

$$\frac{\partial c}{\partial t} + \frac{\rho_b}{n}\frac{\partial s}{\partial t} + \mathbf{v} \cdot \nabla c - \nabla \cdot (\mathbf{D}\nabla c) = -\lambda_{reaction} c \qquad \text{(S.5)}$$

$$\frac{ds}{dt} = \lambda_{sorption}(cK_d - s) \qquad \text{(S.6)}$$

in which c [ML^{-3}] is the aqueous-phase concentration, ρ_b [ML^{-3}] denotes the dry bulk density of the aquifer material, n [-] is effective porosity, s [MM^{-1}] denotes the mass-related concentration of the sorbed compound (mass of the compound per mass of the solids), t [T] is time, $\mathbf{v}$ [LT^{-1}] is the average linear velocity of water, $\mathbf{D}$ [L^2T^{-1}] is the dispersion tensor, $\lambda_{reaction}$ [T^{-1}] expresses the rate coefficient of first-order degradation, $\lambda_{sorption}$ [T^{-1}] is the rate coefficient of first-order mass transfer between the sorbent and the aqueous phases, and

K_d [L^3M^{-1}] is the distribution coefficient of the compound between the sorbing and aqueous phases in equilibrium.

We express the sorbing-phase concentration s by the equivalent aqueous-phase concentration c_* [ML^{-3}] if the two phases were in equilibrium:

$$c_* = \frac{s}{K_d} \tag{S.7}$$

Then, substitution into the preceding equations yields:

$$\frac{\partial c}{\partial t} + \frac{\rho_b}{n} K_d \frac{\partial c_*}{\partial t} + \mathbf{v} \cdot \nabla c - \nabla \cdot (\mathbf{D} \nabla c) = -\lambda_{reaction} c \tag{S.8}$$

$$\frac{dc_*}{dt} = \lambda_{sorption}(c - c_*) \tag{S.9}$$

in which $\frac{\rho_b}{n} K_d$ can be replaced by (R-1), with R [-] being the commonly known retardation factor, which is the mass stored in all phases divided by the mass stored in the aqueous phase if the sorbing and aqueous-phase concentrations are in equilibrium:

$$R = \frac{\rho_b}{n} K_d + 1 \tag{S.10}$$

This results in:

$$\frac{\partial c}{\partial t} + (R - 1) \frac{\partial c_*}{\partial t} + \mathbf{v} \cdot \nabla c - \nabla \cdot (\mathbf{D} \nabla c) = -\lambda_{reaction} c \tag{S.11}$$

to be amended by equation (S.9). In case of instantaneous sorption (i.e., in the limit of $\lambda_{sorption} \to \infty$), the concentrations c and c_* become identical, resulting in the standard retarded advection-dispersion-reaction equation.

As initial condition, we assume for all compounds a concentration of zero:

$$c(t = 0, \mathbf{x}) = 0 \ \forall \mathbf{x} \tag{S.12}$$

We may approximate the multi-dimensional domain as a rectangular box, where the inflow concentration is set to zero in the part of the inflow boundary representing ambient flow and to the time-dependent injected concentration c_{in} [ML^{-3}] at the part of the inflow boundary representing the injection tube. At all other boundaries, we may assume zero dispersive mass flux:

$$\mathbf{n}\cdot(\mathbf{v}c-\mathbf{D}\nabla c)|_{x_1=0}=\begin{cases}\mathbf{n}\cdot\mathbf{v}c_{in}(t) & \text{if} -\frac{w}{2}\le x_3\le\frac{w}{2}\\ 0 & \text{otherwise}\end{cases} \tag{S.13}$$

$$\mathbf{n}\cdot(\mathbf{D}\nabla c)=0 \text{ at all other boundaries} \tag{S.14}$$

in which w [L] is the effective injection height of the injection tube, x_1 is the longitudinal coordinate, and x_3 the vertical.

3.2. Approximation by One-Dimensional Transport Subjected to Dilution by Transverse Dispersion

The governing transport equation is linear with respect to the solute concentration. If we assume that the physical transport coefficients **v** and **D** are identical, we can approximate the simulated breakthrough curve at an observation point by a 1-D model, in which the effect of dilution by transverse dispersion is approximated from conservative steady-state transport of an internal tracer:

$$c_{reac}(t,\mathbf{x}_{obs})=f_{dil}(\mathbf{x}_{obs})\cdot c_{reac}^{1\mathrm{D}}(t,\mathbf{x}_{obs}) \tag{S.15}$$

$$\frac{\partial c_{reac}^{1\mathrm{D}}}{\partial t}+(R-1)\frac{\partial c_{reac,*}^{1\mathrm{D}}}{\partial t}+v\frac{\partial c_{reac}^{1\mathrm{D}}}{\partial x}-D\frac{\partial^2 c_{reac}^{1\mathrm{D}}}{\partial x^2}=-\lambda_{reaction}c_{reac}^{1\mathrm{D}} \tag{S.16}$$

$$\frac{dc_{reac,*}^{1\mathrm{D}}}{dt}=\lambda_{sorption}\left(c_{reac}^{1\mathrm{D}}-c_{reac,*}^{1\mathrm{D}}\right) \tag{S.17}$$

$$c_{reac}^{1\mathrm{D}}(t=0,x)=0 \tag{S.18}$$

$$vc_{reac}^{1\mathrm{D}}-D\frac{\partial c_{reac}^{1\mathrm{D}}}{\partial x}=vc_{in}(t) \text{ at } x=0 \tag{S.19}$$

$$\mathbf{v}\cdot\nabla f_{dil}-\nabla\cdot(\mathbf{D}\nabla f_{dil})=0 \tag{S.20}$$

$$\mathbf{n}\cdot(\mathbf{v}f_{dil}-\mathbf{D}\nabla f_{dil})|_{x_1=0}=\begin{cases}\mathbf{n}\cdot\mathbf{v} & \text{if} -\frac{w}{2}\le x_3\le\frac{w}{2}\\ 0 & \text{otherwise}\end{cases} \tag{S.21}$$

$$\mathbf{n}\cdot(\mathbf{D}\nabla f_{dil})=0 \text{ at all other boundaries} \tag{S.22}$$

This approximation introduces a small error because the dilution due to transverse dispersion is slightly smaller at the rising limb of a tracer breakthrough than at the falling limb, but these transient effects are negligible in practical applications.

Equations (S.20-S.22) contain the spatially variable transport coefficients **v** and **D**. Rather than solving these equations numerically, we obtain the dilution factor from the plateau concentration $c_{int.std.}^{plateau}$ [ML^{-3}] of the internal standard:

$$f_{dil}(\mathbf{x}_{obs}) = \frac{c_{int.std.}^{plateau}(\mathbf{x}_{obs})}{c_{in,int.std.}} \tag{S.23}$$

which implies that we cannot make any statements about transverse dispersion coefficients or the spatial distribution of the velocity field.

3.3. Numerical Methods and Fitting Procedure.

The 1-D transport equations (S.16-S.19) have an analytical solution in the Laplace domain:

$$\tilde{c}_{reac}^{1\mathrm{D}}(s) = \tilde{c}_{in}(s)\frac{v}{v+\alpha D}\exp(-\alpha x) \tag{S.24}$$

$$\alpha = \frac{-v+\sqrt{v^2+4Db}}{2D} \tag{S.25}$$

$$b = s + \frac{(R-1)s\lambda_{sorption}}{s+\lambda_{sorption}} + \lambda_{reaction} \tag{S.26}$$

in which s [T^{-1}] is the Laplace coordinate, and quantities with a tilde are the Laplace transform of the corresponding time function. We have programed these expressions in Matlab and use the numerical inverse Laplace transform of de Hoog et al.[5] to obtain concentration BTC.

The numerical inverse Laplace transformation leads to spurious oscillations deeming the solution too inaccurate for the evaluation of isotope ratios. Thus, for the evaluation of isotope BTCs, we used another Matlab program relying on Finite Volume discretization in space using upstream differentiation for advective transport and a time step size to reach a Courant number of unity. Dispersion was solved implicitly. Subsequently, mass transfer and degradation were solved in a decoupled reaction step using explicit Euler integration. The grid spacing was 0.01m. We considered each isotopologue as an independent species. Because of linearity they do not influence each other. After computing the concentrations of the isotopologues, we evaluated the corresponding isotope ratios using the δ notation.

The dilution factors f_{dil} for D_2O and BAM are obtained by scaling the second-largest concentration value in the corresponding breakthrough curve with the inflow concentration. The apparent velocity v and longitudinal dispersion coefficient D are obtained by fitting the model (without sorption and degradation) to the breakthrough curve of D_2O using the dilution factor already obtained. The degradation coefficients $\lambda_{reaction}$ of bentazone and diclofenac, as well as the sorption coefficients K_d and $\lambda_{sorption}$ of diclofenac are obtained by fitting the corresponding models to the concentration BTCs, using the dilution factor of BAM. These fits are done with the global-search genetic algorithm of the corresponding Matlab toolbox using standard parameters except for the population size, which was set to 1000. The isotope-fractionation factors were manually adjusted.

3.4. Justification of $\alpha_{sorption}^{kin} = 1\ (\varepsilon_{sorption}^{kin} = 0)$

Besides the equilibrium sorption isotope effect, also the rate constant of the sorption process may be subject to (kinetic) isotope effects. Heavy isotopologues would be expected to sorb and desorb more slowly because of their lower diffusion coefficient. The assumption of such a normal kinetic sorption isotope effect was evaluated for sorption of diclofenac with $\varepsilon_{sorption}^{kin} = -1.8\,‰$ (both for carbon and nitrogen isotopologues). Figure S3 shows, however, that the agreement of the model with experimental data got significantly worse. A kinetic isotope effect on sorption was, therefore, not integrated into the model, i.e., $\varepsilon_{sorption}^{kin} = 0\,‰$ was assumed.

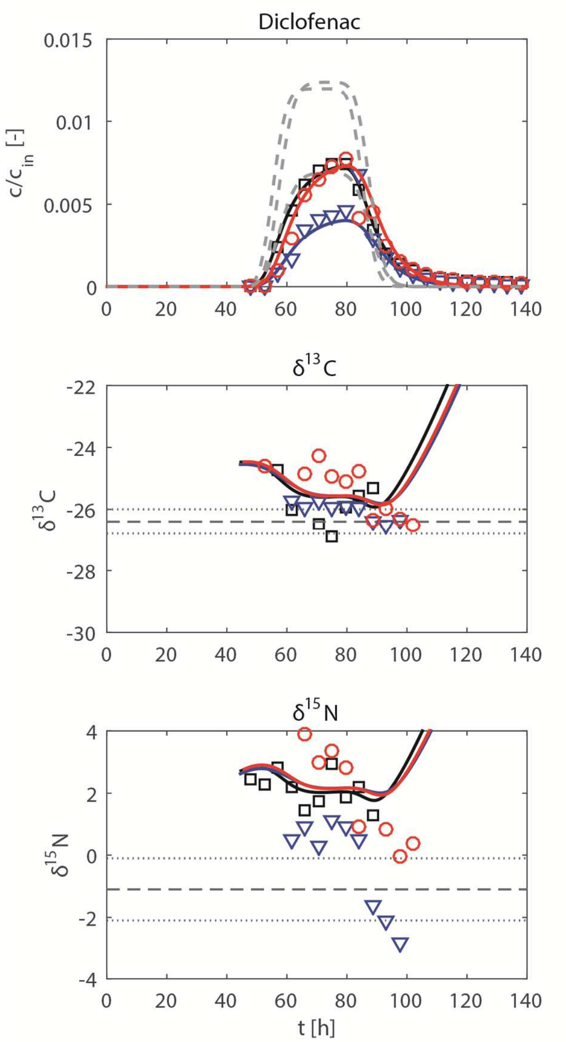

Figure S3. Breakthrough curve of diclofenac assuming a kinetic isotope effect on sorption and desorption of $\varepsilon_{sorption}^{kin} = -1.8\,‰$ (both for carbon and nitrogen isotopologues).

3.5. Plausibility of a dilution factor of BAM on the order of one percent ($f_{dil} \approx 0.01$)

The dilution factor determined for BAM falls in the same order of magnitude as experimentally determined and modelled for bromide in our preceding study.[6,7]

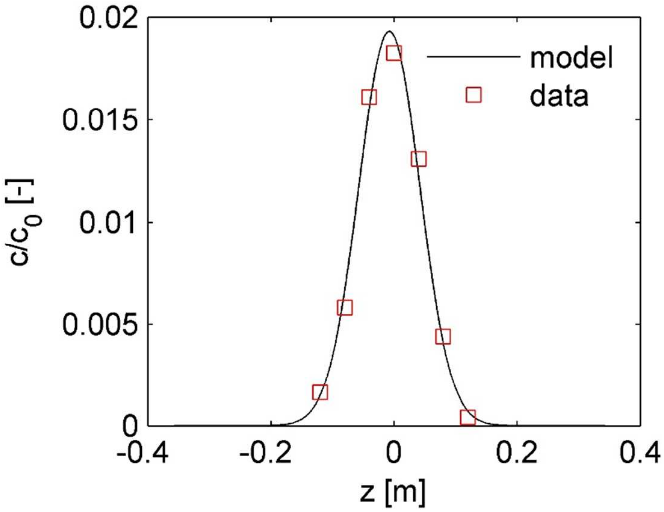

Figure S4. Measured, steady-state bromide concentrations in the physical aquifer model at 4.2 m distance and the model fit used in the preceding toluene study.

3.6. Model Quality

To determine the quality of the model, the normalized root mean square error (NRMSE) was calculated by dividing the root mean square error (RMSE) by the measurement uncertainty (± 0.4‰ (BAM, bentazone) and ± 0.5‰ (diclofenac) for carbon; ± 1‰ for nitrogen) of isotope analysis:

$$NRMSE = \frac{RMSE}{uncertainty} \tag{S.27}$$

with RMSE as

$$RMSE = \sqrt{\frac{\sum_{i=1}^{n}\left(\delta\,^{h}E_{obs,i} - \delta\,^{h}E_{mod,i}\right)^{2}}{n}} \tag{S.28}$$

$\delta^{h}E_{obs,i}$ and $\delta^{h}E_{mod,i}$ are the measured and modeled isotope values of carbon and nitrogen, respectively, and n is the number of data points.

Table S3. (Normalized) root mean square errors ((N)RMSE) of BAM, bentazone, and diclofenac isotope analysis for the sampling ports F 1-3, F 3-3, and F 3-4.

		sampling ports		
		F 1-3	**F 3-3**	**F 3-4**
	BAM	0.421	0.200	0.287
	bentazone	0.556	0.601	0.308
RMSE$_{carbon}$ [‰]	**diclofenac (combined)**	0.901	0.646	0.577
	diclofenac (degr. only)	0.936	0.687	0.731
	diclofenac (sorp. only)	1.046	0.361	1.206
	BAM	1.052	0.501	0.718
	bentazone	1.390	1.503	0.771
NRMSE$_{carbon}$ [ ]	**diclofenac (combined)**	1.803	1.292	1.153
	diclofenac (degr. only)	1.871	1.375	1.463
	diclofenac (sorp. only)	2.091	0.722	2.412
	BAM	0.754	0.375	0.985
	bentazone	2.761	2.261	2.413
RMSE$_{nitrogen}$ [‰]	**diclofenac (combined)**	0.960	2.148	1.105
	diclofenac (degr. only)	0.664	2.591	1.587
	diclofenac (sorp. only)	2.954	1.378	3.991
	BAM	0.754	0.375	0.985
	bentazone	2.761	2.261	2.413
NRMSE$_{nitrogen}$ [ ]	**diclofenac (combined)**	0.960	2.148	1.105
	diclofenac (degr. only)	0.664	2.591	1.587
	diclofenac (sorp. only)	2.954	1.378	3.991

4. References

1. Reinnicke, S.; Simonsen, A.; Sørensen, S. R.; Aamand, J.; Elsner, M.; C and N Isotope Fractionation during Biodegradation of the Pesticide Metabolite 2,6-Dichlorobenzamide (BAM): Potential for Environmental Assessments, *Environ. Sci. Technol.* **2012**, *46* (3), 1447-1454.
2. Reinnicke, S.; Bernstein, A.; Elsner, M.; Small and Reproducible Isotope Effects during Methylation with Trimethylsulfonium Hydroxide (TMSH): A Convenient Derivatization Method for Isotope Analysis of Negatively Charged Molecules, *Analytical Chemistry* **2010**, *82* (5), 2013-2019.
3. Maier, M. P.; De Corte, S.; Nitsche, S.; Spaett, T.; Boon, N.; Elsner, M.; C & N Isotope Analysis of Diclofenac to Distinguish Oxidative and Reductive Transformation and to Track Commercial Products, *Environmental Science & Technology* **2014**, *48* (4), 2312-2320.
4. Maier, M. P.; Qiu, S.; Elsner, M.; Enantioselective stable isotope analysis (ESIA) of polar herbicides, *Analytical and Bioanalytical Chemistry* **2013**, *405* (9), 2825-2831.
5. Hoog, F. R. d.; Knight, J. H.; Stokes, A. N.; An improved method for numerical inversion of Laplace transforms, *S.I.A.M. J. Sci. Stat. Comput.* **1982**, *3*, 357-366.
6. Qiu, S.; Eckert, D.; Cirpka, O. A.; Huenniger, M.; Knappett, P.; Maloszewski, P.; Meckenstock, R. U.; Griebler, C.; Elsner, M.; Direct Experimental Evidence of Non-first Order Degradation Kinetics and Sorption-Induced Isotopic Fractionation in a Mesoscale Aquifer: 13C/12C Analysis of a Transient Toluene Pulse, *Environmental Science & Technology* **2013**, *47* (13), 6892-6899.
7. Eckert, D.; Qiu, S.; Elsner, M.; Cirpka, O. A.; Model Complexity Needed for Quantitative Analysis of High Resolution Isotope and Concentration Data from a Toluene-Pulse Experiment, *Environmental Science & Technology* **2013**, *47* (13), 6900-6907.